Switching of Co Magnetization Driven by Antiferromagnetic-Ferromagnetic Phase Transition of FeRh Alloy in Co/FeRh Bilayers

P. Dróżdż,[1,*] M. Ślęzak,[1] K. Matlak,[1] B. Matlak,[1] K. Freindl,[2] D. Wilgocka-Ślęzak,[2] N. Spiridis,[2] J. Korecki,[1,2] and T. Ślęzak[1]

[1]*AGH University of Science and Technology, Faculty of Physics and Applied Computer Science, aleja Adama Mickiewicza 30, 30-059 Kraków, Poland*

[2]*Jerzy Haber Institute of Catalysis and Surface Chemistry, Polish Academy of Sciences, 30-239 Kraków, Poland*

(Received 12 August 2017; revised manuscript received 23 November 2017; published 27 March 2018)

We show that Co spins in Co/FeRh epitaxial bilayers grown on W(110) switch reversibly between the two orthogonal in-plane directions as the FeRh layer undergoes temperature-driven antiferromagnetic-ferromagnetic (AFM-FM) phase transition. The switching of Co magnetization is characterized by a hysteretic behavior owing to a temperature hysteresis of the AFM-FM transition in FeRh. The spin reorientation of Co is driven by the evolution interfacial exchange coupling to the FeRh system across the AFM-FM process. Our results provide a method of writing information purely by a local temperature change.

DOI: 10.1103/PhysRevApplied.9.034030

I. INTRODUCTION

Control of the spin direction in magnetic nanostructures has become a key objective of investigations in nanomagnetism because it is a mandatory requirement for magnetic recording applications. Typically, in ultrathin ferromagnetic films, the magnetization orientation can be tuned in a process of a spin-reorientation transition (SRT), which involves thickness- or temperature-driven switching of the spontaneous magnetization orientation between two directions [1–3]. In our paper, we show a mechanism for reversible in-plane magnetization switching of ferromagnets in contact with FeRh alloy. A FeRh alloy with an equiatomic composition has revealed a temperature-induced first-order magnetic transition from an antiferromagnetic (AFM) to ferromagnetic (FM) state at a transition temperature (T_T) 350 K and a second-order transition to a paramagnetic state at $T_C = 675$ K [4]. This unique AFM-FM magnetic transition (termed "metamagnetic") was first discovered in 1938 [5,6] and is accompanied by volume expansion [7,8], a decrease of resistivity [4], and a large change in entropy [9,10]. Recently, FeRh films exhibiting AFM-FM transitions have attracted considerable attention [11–15], owing to their potential applications in new storage media, such as heat-assisted magnetic recording (HAMR) [16,17]. Our experiments show that in Co/FeRh bilayers grown on W(110), spins of the epitaxial Co films switch reversibly between two orthogonal in-plane directions, namely, $[1\bar{1}0]$ and [001], as the FeRh system undergoes an AFM-FM phase transition. Switching of Co magnetization is realized purely by variation of the temperature, and it is induced by a change of the magnetic coupling between the Co and FeRh spin systems that accompanies the AFM-FM phase transition. The temperature-driven switching of the Co spins is characterized by a hysteretic behavior originating from the intrinsic temperature hysteresis of the AFM-FM phase transition in the FeRh system. The phenomenon reported here goes beyond the HAMR concept consisting in temperature modulation of the coercivity [18] and provides a mechanism for writing information purely by changing the local temperature, which can be realized by laser heating or an electrical current flow.

II. EXPERIMENTAL DETAILS AND STRUCTURAL STUDIES

The ultrathin epitaxial FeRh layer with a thickness of 50 Å is grown by molecular beam epitaxy (MBE) on a W(110) substrate via elemental codeposition at room temperature (the pressure during the deposition is 5×10^{-10} mbar). The nominal Rh atomic concentration is approximately 54%. The sample is postannealed at 800 K for 30 min to promote formation of the desired $B2$structure [19]. The epitaxial character of the FeRh film is confirmed by high-quality low-energy electron-diffraction (LEED) patterns, as shown in Fig. 1(b), together with a LEED pattern corresponding to the W(110) substrate [Fig. 1(a)] and Co overlayer [Fig. 1(c)]. Moreover, by following the thermal evolution of FeRh surface LEED patterns, the temperature dependence of the in-plane lattice constants is derived (see the Supplemental Material [20]). The FeRh lattice parameters are within accuracy of the temperature-independent LEED analysis, proving that the FeRh surface structure is stable across the AFM-FM phase transition.

*piotr.drozdz@fis.agh.edu.pl

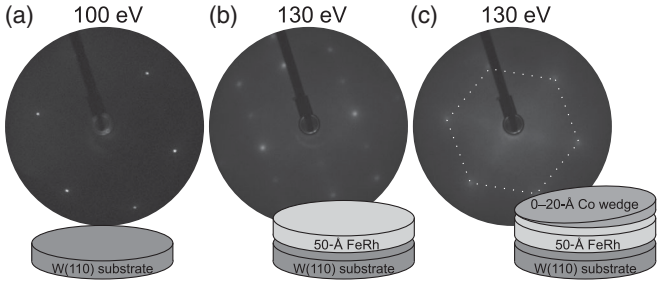

FIG. 1. LEED patterns of (a) W(110) single-crystal surface, (b) FeRh alloy film, and (c) cobalt deposited on a FeRh system. White dotted line indicates the regular hexagon which marks the positions of the diffraction spots. Energy of incident electrons is given above the images.

The magnetic properties are studied *in situ* by the longitudinal magneto-optical Kerr effect (LMOKE). We use a standard optical layout for the LMOKE setup with *s*-polarized light ($\lambda = 635$ nm) and photoelastic modulator ($f = 50$ kHz) with lock-in detection. The $2f$ signal measured by the detector is proportional to the Kerr rotation [21].

III. MAGNETIC PROPERTIES AND DISCUSSION

To obtain the temperature dependence of magnetization, LMOKE magnetic hysteresis loops are measured over a wide temperature range and normalized to the highest value of the measured Kerr rotation at saturation $\mathrm{ROT_{sat}}$ [corresponding to the loop collected at 330 K during the cooling process shown in Fig. 2(a)]. The $\mathrm{ROT_{sat}}$ obtained from normalized loops is taken as a measurement of the saturation magnetization. The exemplary hysteresis loops

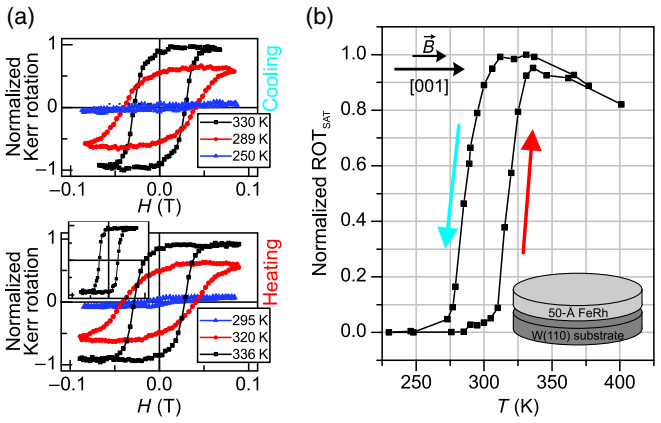

FIG. 2. (a) The exemplary LMOKE magnetic hysteresis loops acquired with external magnetic field applied along the [001] direction, across the AFM-FM phase transition for a 50-Å-thick FeRh film on W(110) for the heating and cooling transition branches. Inset in the bottom panel shows the loop collected for 350 K with external magnetic field applied along the $[1\bar{1}0]$ direction. The external magnetic field and Kerr rotation axes in the inset have the same scale as in the main figure. (b) Temperature magnetization profile of the AFM-FM phase transition.

recorded with the external magnetic field applied parallel to the [001] in-plane direction of W(110) during the cooling and heating processes together with the corresponding temperature magnetization profile of the AFM-FM phase transition are shown in Fig. 2.

The critical transition temperatures of the heating and cooling branches are estimated to be $T_{\mathrm{heat}} = 318$ K and $T_{\mathrm{cool}} = 286$ K, respectively, resulting in a transition hysteresis of $\Delta T = 32$ K. The transition is clearly shifted toward lower temperatures compared with that of the bulk FeRh system ($T_{\mathrm{heat}} = 360$ K, $T_{\mathrm{cool}} = 345$ K [4]), and its hysteresis is broader. Our systematic studies of the thickness dependence of the AFM-FM transition (data not shown) indicate that the major effect on the transition temperature is a lattice strain originated from the considerable mismatch between the W(110) substrate and the FeRh system. This effect allows tailoring of both the critical transition temperature and the hysteresis shape by changing the FeRh film thickness. The in-plane magnetic anisotropy of the discussed FeRh film in the FM phase is small, as indicated by the similar LMOKE results obtained with an external magnetic field applied along the in-plane $[1\bar{1}0]$ direction [see the inset in the bottom panel of Fig. 2(a)].

On top of the FeRh alloy film, a wedge-shaped Co layer with a thickness varying from 0 to 20 Å is grown by MBE at room temperature with the use of a shutter moving in front of the sample during the Co deposition. The deposition of cobalt is followed by annealing at 500 K for 15 min. The LEED pattern corresponding to the Co surface shown in Fig. 1(c) with a regular hexagon tailored to the positions of the diffraction spots indicates that the Co crystallized on the FeRh (110) plane in a hexagonal hcp phase. Moreover, the LEED patterns measured at specific electron energies are very similar over the whole examined Co thickness range, indicating that the hexagonal symmetry of the Co film surface is preserved over the entire thickness range.

The Co growth is followed by *in situ* temperature- and Co thickness-dependent LMOKE measurements with external magnetic fields applied along the $[1\bar{1}0]$ and [001] in-plane directions. Figure 3 shows representative hysteresis loops measured for the two distinct Co thicknesses $d_{\mathrm{Co}} = 6$ Å and $d_{\mathrm{Co}} = 13$ Å at 350 K. This temperature corresponds to the FM state of the FeRh alloy denoted as $\mathrm{FeRh_{FM}}$ and 130 K corresponding to the AFM state of the FeRh alloy denoted as $\mathrm{FeRh_{AFM}}$. The insets in the bottom panel of Fig. 3 show corresponding loops measured at 130 K with an external field applied along the [001] direction.

The hysteresis loops measured at 350 K with an external magnetic field along the $[1\bar{1}0]$ direction for both thicknesses (top panel of Fig. 3) are rectangular, indicating that the easy magnetization direction lies along the $[1\bar{1}0]$ direction. This is confirmed by the typical hard axis loops measured with external magnetic field applied in the [001]

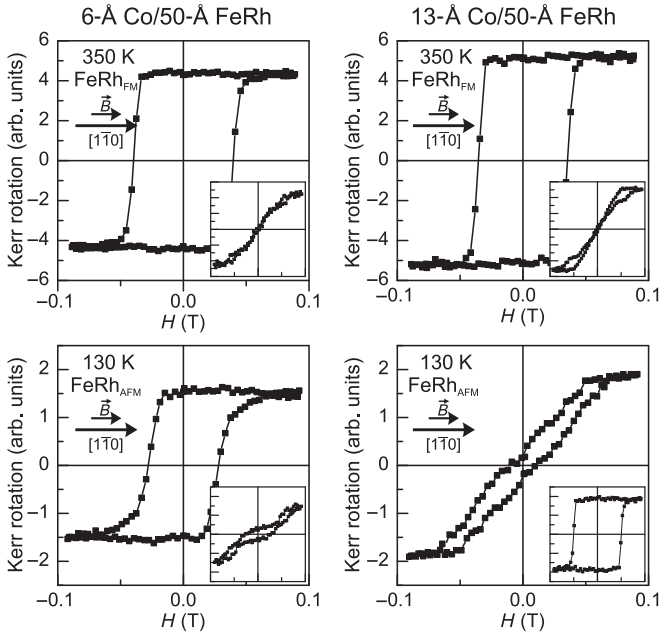

FIG. 3. LMOKE loops measured for the Co/FeRh bilayer with an external magnetic field applied along the $[1\bar{1}0]$ in-plane direction shown for cobalt film thicknesses of 6 Å (left panel) and 13 Å (right panel). The top and bottom panels correspond to measurements at 350 and 130 K, respectively. Insets show LMOKE loops measured along the [001] direction. The external magnetic field axis in the insets has the same scale as in the main figures.

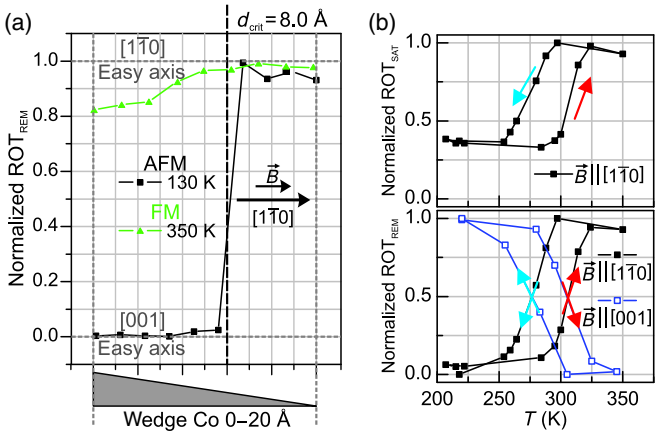

FIG. 4. (a) Remanence Kerr rotation $\mathrm{ROT_{REM}}$ normalized to the saturation determined from LMOKE loops measured with external magnetic field applied along the $[1\bar{1}0]$ direction shown as a function of the cobalt thickness. (b) Temperature dependence of the saturation Kerr rotation $\mathrm{ROT_{SAT}}$ and remanence Kerr rotation $\mathrm{ROT_{REM}}$ determined from LMOKE loops measured with external magnetic field applied along the $[1\bar{1}0]$ and [001] directions shown as a function of the temperature for $d_{\mathrm{Co}} = 13$ Å.

direction (see insets in the top panel of Fig. 3). However, at lower temperatures, the magnetic anisotropy clearly changes the orientation of the easy axis to the [001] direction for $d_{\mathrm{Co}} = 13$ Å, while the $[1\bar{1}0]$ direction remains easy for $d_{\mathrm{Co}} = 6$ Å. This can be clearly seen from the shape of the loops measured for the $[1\bar{1}0]$ and [001] directions, respectively (see the insets in the bottom panel of Fig. 3). The hard axis loops observed at 130 K for $d_{\mathrm{Co}} = 6$ Å along the [001] direction and $d_{\mathrm{Co}} = 13$ Å along the $[1\bar{1}0]$ direction are characterized by a low-remanence and high-saturation magnetic field. These findings indicate a thickness-driven SRT at 130 K.

The systematic LMOKE measurements performed as a function of the Co thickness at 130 and 350 K allow us to derive the dependence of the remanence Kerr signal $\mathrm{ROT_{rem}}$ as a function of the Co thickness, as shown in the Fig. 4(a) for the discussed temperatures. At 350 K, the saturation-normalized remanence signal derived from the $[1\bar{1}0]$ loops is only weakly temperature dependent and close to unity. Additionally, the remanence signal for the [001] direction is nearly zero at all cobalt thicknesses (data not shown). This finding indicates that the easy magnetization axis of the Co/FeRh system at 350 K is along the $[1\bar{1}0]$ direction over the whole investigated thickness range. In contrast to the 350-K behavior, at 130 K the remanence derived from the $[1\bar{1}0]$ loops decreases from nearly 1 at a low thickness to zero for cobalt thicker than $d_{\mathrm{crit}} = 8$ Å. This behavior is accompanied by an inverse change of the remanence derived from LMOKE loops along the [001] direction, indicating that at low temperatures corresponding to the AFM state of FeRh, the cobalt layer undergoes a thickness-driven in-plane SRT. Moreover, a comparison of the LMOKE remanence thickness dependence between the two discussed temperatures clearly indicates that cobalt thicker than $d_{\mathrm{crit}} = 8$ Å features a temperature-driven SRT between the $[1\bar{1}0]$ direction at 350 K and the [001] direction at 130 K.

To understand the origin of the observed SRT, we perform a temperature-dependent LMOKE measurement for a selected Co thickness in the range above d_{crit} of thickness-driven SRT at 130 K, namely, for $d_{\mathrm{Co}} = 13$ Å. The LMOKE loops are measured with an external field applied along the $[1\bar{1}0]$ and [001] directions during the temperature cycle 350 K $\Rightarrow$ 200 K $\Rightarrow$ 350 K. The amplitude of the LMOKE signal $\mathrm{ROT_{SAT}}$ corresponding to the saturation state [Fig. 4(b) top panel] and the normalized remanence Kerr rotation $\mathrm{ROT_{REM}}$ [Fig. 4(b) bottom panel] are determined as a function of the temperature.

The temperature evolution of the saturation Kerr signal corresponds to the AFM-FM phase transition in the FeRh and is characterized by a typical transition-temperature hysteresis. The critical transition temperatures on heating and cooling branches are estimated to be $T_{\mathrm{heat}} = 308$ K and $T_{\mathrm{cool}} = 274$ K, respectively, resulting in a transition hysteresis $\Delta T = 34$ K. The transition is shifted by approximately 10 K toward lower temperatures compared with that of the uncoated FeRh film. We are inclined to attribute this shift to the exchange coupling with the ferromagnetic

cobalt film, but it can also be caused by possible interdiffusion at the Co/FeRh interface. In parallel, the remanence Kerr signal is a fingerprint of the magnetization orientation, and its temperature-induced evolution is a manifestation of the cobalt SRT between the $[1\bar{1}0]$ direction (high remanence value) and [001] direction (low remanence state). It is clear from a comparison of the bottom and top panels of Fig. 4(b) that the temperature-driven SRT is characterized by an identical hysteresis to that of the AFM-FM phase transition. Thus, we consider that the SRT is induced by the phase transition of the alloy film. This observation shows that by changing the temperature of the Co/FeRh bilayer, the 90° magnetization switching can be realized without any additional external factor as an external magnetic field or electric current. With this effect, one can imagine writing information bits represented by Co magnetization orientation. The homogenous [001] magnetization state after cooling the system below T_{cool} represents the overwritten or erased state of our medium. Writing of the information bit (reorienting magnetization to the $[1\bar{1}0]$ state) requires heating of the system above T_{heat} that possibly can be realized by the laser heating as the AFM-FM transition can be induced in that way [22]. The stability of the information is ensured by the hysteresis of the AFM-FM transition that governs the hysteresis in Co SRT, as shown in Fig. 4(b). Moreover, stored information is not only thermally protected, but it also becomes insensitive to the external magnetic fields as the magnetic fields required to influence the AFM-FM transition are relatively high [12,23]. Overwriting or erasing of the bit requires cooling below T_{cool}. The cooling erases the information in all bits, suggesting the proposed system is suitable for the erasable and programmable read-only nonvolatile memories with the special feature of the pure temperature-driven information storage. Our interpretation of the observed SRT involves the intrinsic uniaxial anisotropy of the FeRh/Co interface with an easy axis parallel to the $[1\bar{1}0]$ direction. This conclusion is supported by the LMOKE loops measured for the whole investigated Co thickness range at temperatures above $T_{\mathrm{AFM\text{-}FM}}$ and at low temperatures for the low-cobalt-thickness regime. Furthermore, along with the AFM-FM phase transition, a change between a frustrated and collinear interlayer exchange coupling Co-FeRh takes place for the $\mathrm{FeRh_{AFM}}$ and $\mathrm{FeRh_{FM}}$ states, respectively. In the $\mathrm{FeRh_{AFM}}$ state, the cobalt spins cannot simultaneously satisfy the parallel alignment to the opposite Fe spin sublattices of the compensated (110) FeRh plane, which leads to the spin-flop phenomena. This frustration results in an abrupt switching of the Co magnetization to the [001] direction, which is perpendicular to the Fe spins in a FeRh system. Consequently, a lack of an exchange bias is observed in our LMOKE data, in agreement with the findings of Schulthess and Butler [24] and Moran *et al.* [25] for the $\mathrm{FeF_2/Fe}$ system. A schematic drawing of the evolution of the interfacial spin structure across the FM-AFM transition for FeRh covered by Co is shown in Fig. 5.

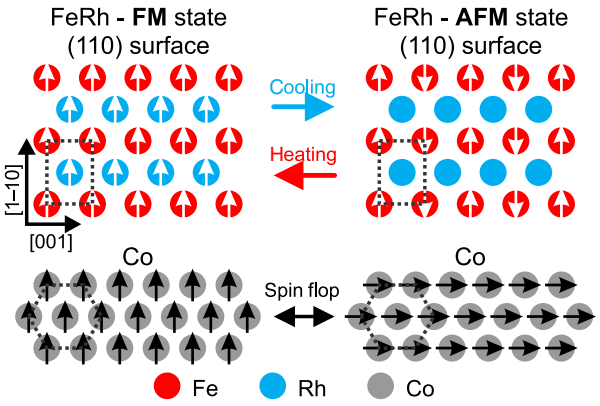

FIG. 5. Schematic showing the evolution of the interfacial spin structure across the FM-AFM transition for the Co/FeRh bilayer for $d_{\mathrm{Co}} = 13$ Å. Left and right panels correspond to the $\mathrm{FeRh_{FM}}$ and $\mathrm{FeRh_{AFM}}$ states of the alloy film, respectively. White and black arrows label the FeRh (red and blue spheres) and Co (gray spheres) spins, respectively.

Finally, the origin of the thickness-induced cobalt SRT at low temperatures can be interpreted in a similar way. In the low-thickness limit, interfacial contributions preferring the $[1\bar{1}0]$ magnetization direction are stronger than the spin-flop-induced uniaxial magnetic anisotropy. Thus, the magnetization aligns parallel to the $[1\bar{1}0]$ direction. The origin of the uniaxial magnetic anisotropy that explains the spin-flop phenomenon has been proposed by Schulthess and Butler [24]. They showed that such anisotropy is responsible for the large coercivity of the easy-axis hysteresis curves that is observed also in our case (compare the wide rectangular hysteresis curve measured along the [001] direction at 130 K shown in the inset of Fig. 3). As the thickness increases, the two anisotropic contributions compete. However, the relative impact of the FeRh/Co interface anisotropy decreases with increasing cobalt thickness, and above d_{crit}, the spin-flop-induced anisotropy dominates, forcing the reorientation transition to the [001] direction. We like to underline that although the control of the in-plane spin-reorientation process has been reported by a several authors [1–3,26–28], the mechanism responsible for the reported Co SRT, namely, the evolution of interfacial exchange interaction accompanying the FeRh phase transition, is original and results in the additional feature of the temperature-driven SRT process, such as its thermal hysteresis. In a classical understanding of SRT that involves the competition between various magnetic anisotropy contributions, no hysteresis is expected.

IV. CONCLUSION

In conclusion, we show that it is possible to write an information bit (represented by the Co magnetization

orientation) in FeRh/Co bilayers by a temperature change alone. Such simple magnetization switching is possible owing to a temperature-driven AFM-FM phase transition in the FeRh layer. Our observations indicate the possibility of using the AFM-FM phase transitions in a device (heat engine) that transfers the thermal energy to the magnetic anisotropy energy of a ferromagnetic system neighboring the FeRh layer. The integration of a FeRh system with a properly designed sandwichlike system might result in a manipulation of the magnetization direction of ferromagnetic sublayers in a multilayer stack or even a whole multilayer that is important for spintronic application.

ACKNOWLEDGMENTS

This work is supported by the National Science Center Poland under Project No. 2015/19/B/ST3/00543 and partially by the AGH University of Science and Technology statutory task No. 11.11.220.01/6 within subsidy of the Ministry of Science and Higher Education.

[1] P. J. Jensen and K. H. Bennemann, Magnetic structure of films: Dependence on anisotropy and atomic morphology, Surf. Sci. Rep. **61**, 129 (2006).

[2] H. P. Oepen, M. Speckmann, Y. Millev, and J. Kirschner, Unified approach to thickness-driven magnetic reorientation transitions, Phys. Rev. B **55**, 2752 (1997).

[3] S. Hope, E. Gu, B. Choi, and J. A. C. Bland, Spin Engineering in Ultrathin Cu/Co/Cu(110), Phys. Rev. Lett. **80**, 1750 (1998).

[4] J. S. Kouvel and C. C. Hartelius, Anomalous magnetic moments and transformations in the ordered alloy FeRh, J. Appl. Phys. **33**, 1343 (1962).

[5] M. Fallot, Les Alliages Du Fer Avec Les Métaux de La Famille Du Platine, Ann. Phys. (Paris) **11**, 291 (1938).

[6] M. Fallot and R. Hocart, Sur L'apparition Du Ferromagnétisme Par Élévation de Température Dans Des Alliages de Fer et de Rhodium, Rev. Sci. **77**, 498 (1939).

[7] A. I. Zakharov, A. M. Kadomtseva, R. Z. Levitin, and E. G. Ponyatovskii, Magnetic and magnetoelastic properties of a metamagnetic iron-rhodium alloy, Sov. Phys. JETP **19**, 1348 (1964).

[8] M. R. Ibarra and P. A. Algarabel, Giant volume magnetostriction in the FeRh alloy, Phys. Rev. B **50**, 4196 (1994).

[9] J. S. Kouvel, Unusual nature of the abrupt magnetic transition in FeRh and its pseudobinary variants, J. Appl. Phys. **37**, 1257 (1966).

[10] M. P. Annaorazov, S. A. Nikitin, A. L. Tyurin, K. A. Asatryan, and A. K. Dovletov, Anomalously high entropy change in FeRh alloy, J. Appl. Phys. **79**, 1689 (1996).

[11] R. O. Cherifi, V. Ivanovskaya, L. C. Phillips, A. Zobelli, I. C. Infante, E. Jacquet, V. Garcia, S. Fusil, P. R. Briddon, N. Guiblin, A. Mougin, A. A. Ünal, F. Kronast, S. Valencia, B. Dkhil, A. Barthélémy, and M. Bibes, Electric-field control of magnetic order above room temperature, Nat. Mater. **13**, 345 (2014).

[12] X. Marti, I. Fina, C. Frontera, J. Liu, P. Wadley, Q. He, R. J. Paull, J. D. Clarkson, J. Kudrnovský, I. Turek, J. Kuneš, D. Yi, J. Chu, C. T. Nelson, L. You, E. Arenholz, S. Salahuddin, J. Fontcuberta, T. Jungwirth, and R. Ramesh, Room-temperature antiferromagnetic memory resistor, Nat. Mater. **13**, 367 (2014).

[13] C. Bordel, J. Juraszek, D. W. Cooke, C. Baldasseroni, S. Mankovsky, J. Minar, H. Ebert, S. Moyerman, E. E. Fullerton, and F. Hellman, Fe Spin Reorientation across the Metamagnetic Transition in Strained FeRh Thin Films, Phys. Rev. Lett. **109**, 117201 (2012).

[14] Y. Lee, Z. Q. Liu, J. T. Heron, J. D. Clarkson, J. Hong, C. Ko, M. D. Biegalski, U. Aschauer, S. L. Hsu, M. E. Nowakowski, J. Wu, H. M. Christen, S. Salahuddin, J. B. Bokor, N. A. Spaldin, D. G. Schlom, and R. Ramesh, Large resistivity modulation in mixed-phase metallic systems, Nat. Commun. **6**, 5959 (2015).

[15] C. Stamm, J. U. Thiele, T. Kachel, I. Radu, P. Ramm, M. Kosuth, J. Minár, H. Ebert, H. A. Dürr, W. Eberhardt, and C. H. Back, Antiferromagnetic-ferromagnetic phase transition in FeRh probed by x-ray magnetic circular dichroism, Phys. Rev. B **77**, 184401 (2008).

[16] J. Thiele, S. Maat, and E. E. Fullerton, FeRh/FePt exchange spring films for thermally assisted magnetic recording media, Appl. Phys. Lett. **82**, 2859 (2003).

[17] M. H. Kryder, E. C. Gage, T. W. Mcdaniel, W. a. Challener, R. E. Rottmayer, G. Ju, Y. T. Hsia, and M. F. Erden, Heat assisted magnetic recording, Proc. IEEE **96**, 1810 (2008).

[18] N. T. Nam, W. Lu, and T. Suzuki, Exchange bias of ferromagnetic/antiferromagnetic in FePt/FeRh bilayers, J. Appl. Phys. **105**, 07D708 (2009).

[19] S. K. Kim, Y. Tian, F. Jona, and P. M. Marcus, Atomic structure of a {110} surface of the FeRh alloy, Phys. Rev. B **56**, 9858 (1997).

[20] See Supplemental Material at http://link.aps.org/supplemental/10.1103/PhysRevApplied.9.034030 for details of the structure analysis.

[21] P. Vavassori, Polarization modulation technique for magneto-optical quantitative vector magnetometry, Appl. Phys. Lett. **77**, 1605 (2000).

[22] G. Ju, J. Hohlfeld, B. Bergman, R. J. M. van de Veerdonk, O. N. Mryasov, J. Y. Kim, X. Wu, D. Weller, and B. Koopmans, Ultrafast Generation of Ferromagnetic Order via a Laser-Induced Phase Transformation in FeRh Thin Films, Phys. Rev. Lett. **93**, 197403 (2004).

[23] S. Inoue, H. Y. Y. Ko, and T. Suzuki, Magnetic properties of single-crystalline FeRh alloy thin films, IEEE Trans. Magn. **44**, 2875 (2008).

[24] T. C. Schulthess and W. H. Butler, Consequences of Spin-Flop Coupling in Exchange Biased Films, Phys. Rev. Lett. **81**, 4516 (1998).

[25] T. J. Moran, J. Nogués, D. Lederman, I. K. Schuller, D. Lederman, and I. K. Schuller, Perpendicular coupling at interfaces perpendicular coupling at Fe-FeF_2 interfaces, Appl. Phys. Lett. **72**, 617 (1998).

[26] T. Ślęzak, M. Ślęzak, M. Zając, K. Freindl, A. Kozioł-Rachwał, K. Matlak, N. Spiridis, D. Wilgocka-Ślęzak, E. Partyka-Jankowska, M. Rennhofer, A. I. Chumakov, S. Stankov, R. Rüffer, and J. Korecki, Noncollinear Magnetization Structure at the Thickness-Driven Spin-Reorientation

Transition in Epitaxial Fe Films on W(110), Phys. Rev. Lett. **105**, 027206 (2010).

[27] M. Ślęzak, T. Giela, D. Wilgocka-Ślęzak, A. Kozioł-Rachwał, T. Ślęzak, R. Zdyb, N. Spiridis, C. Quitmann, J. Raabe, N. Pilet, and J. Korecki, X-ray photoemission electron microscopy study of the in-plane spin reorientation transitions in epitaxial Fe films on W(110), J. Magn. Magn. Mater. **348**, 101 (2013).

[28] Y. Millev and J. Kirschner, Reorientation transitions in ultrathin ferromagnetic films by thickness- and temperature-driven anisotropy flows, Phys. Rev. B **54**, 4137 (1996).